Developmental Biology **227,** 324–342 (2000)
doi:10.1006/dbio.2000.9915, available online at http://www.idealibrary.com on IDEAL®

The Murine Gene, *Traube*, Is Essential for the Growth of Preimplantation Embryos

Tim Thomas,[1,2] Anne K. Voss,[1,2,3] Petros Petrou, and Peter Gruss

Max-Planck-Institute of Biophysical Chemistry, Department of Molecular Cell Biology, Am Fassberg 11, 37077 Goettingen, Germany

Little is known about the genetic control of preimplantation development. We have isolated, characterized, and mutated a previously undescribed mouse gene, *Traube (Trb),* essential for preimplantation development. Similar protein coding sequences are found in rats, humans, and yeast. The TRB protein contained two amino-terminal acidic domains, a leucine zipper, and three putative nuclear localization signals. The *Trb* gene was expressed at low levels ubiquitously early in development and became restricted to the liver and the central nervous system from E11.5 onward. Myc-tagged TRB protein was localized to the nucleus, and in a large proportion of the cells to the nucleoli. The *Trb* mutant embryos halted in development at the compacted morula stage at E2.5. At E3.5 they started to decompact and a day later they disintegrated and died. The observed defect was cell autonomous, as mutant cells failed to participate in the formation of chimeric embryos. The *Trb* mutant embryos showed a 50% reduction of the total cell number. The mutant embryos exhibited a paucity of ribosomes, polyribosomes, and rough endoplasmic reticulum. This paucity of ribosomes together with the localization of TRB to the nucleoli, the site of ribosome synthesis, suggests that TRB is involved in the synthesis of ribosomes.

Key Words: **morula; preimplantation development; embryonic genome activation; nuclear protein.**

INTRODUCTION

Mammalian preimplantation development is characterized by a series of cell divisions occurring essentially without an increase in mass. For the first stage in this process, stores of maternal RNA and proteins accumulated during oogenesis are utilized to accommodate the specific requirements of the preimplantation embryo. A critical step in mouse embryo development occurs at the 2-cell stage when the embryonic genome is activated, although some embryonic genes are expressed at the 1-cell stage (Flach *et al.*, 1982; Latham, 1999). At this point the embryo acquires the ability to regulate its own development. At the 8-cell stage individual blastomeres of the embryo have the capacity to form all cells of the embryo and all extraembryonic tissues of the conceptus (Kelly, 1977). At the late 8-cell stage the surfaces of the blastomeres flatten to each other and cell adherence complexes and tight junctions are formed. In the compacted morulae the first lineage restriction occurs. The outer polarized cells form trophoblasts and the inner apolar cells become inner cell mass cells which will form the embryo proper as well as some of the extraembryonic tissues.

In particular, the cell adherence complex proteins have been shown to be important for the compaction process. Antibodies against E-cadherin prevent embryos from compacting (Ekblom *et al.*, 1986). Cadherin-mediated cell interactions are calcium dependent and withdrawal of calcium leads to decompaction (Ducibella and Anderson, 1975). Murine embryos carrying a mutation in the *E-cadherin* gene initially compact and then decompact without formation of a blastocoel cavity (Larue *et al.*, 1994; Riethmacher *et al.*, 1995). *α-E-catenin* mutants initially compact and form blastocysts. However, compaction is not maintained. The blastocoels collapse and the embryos do not hatch from their zonae pellucidae (Torres *et al.*, 1997). Placed in culture, the *E-cadherin* and the *α-E-catenin* mutant embryos give rise to cell lines. Only loose association between individual cells of these cell lines was observed (*Larue et al.*, 1994; Torres *et al.*, 1997). Tight junctions and desmo-

[1] The first and second authors contributed equally to this study.

[2] Current address: Development and Neurobiology, The Walter and Eliza Hall Institute of Medical Research, Royal Parade, Parkville, Victoria 3050, Australia.

[3] To whom correspondence should be addressed. E-mail: avoss@wehi.edu.au.

0012-1606/00 $35.00

somes are formed in the E-cadherin-deficient embryos at the areas of distorted cell-cell contact (Riethmacher *et al.*, 1995). In addition to adherence junctions, efficient gap junctional communication appears to be necessary for the maintenance of compaction (Lee *et al.*, 1987; Becker *et al.*, 1992). When antibodies against gap junctional proteins are injected into murine E0.5 embryos, gap junctional communication is disturbed and these embryos fail to compact. However, they continue to divide (Lee *et al.*, 1987). Lack of desmosomal proteins studied so far have not caused preimplantation lethalities (Ruiz *et al.*, 1996; Koch *et al.*, 1997). These studies indicate that cell adhesion complexes and gap junctions are indispensable for compaction and/or the maintenance of compaction and, so, for blastocysts formation, but they are not required for cell survival or cell proliferation. These proteins are present in the embryo before compaction, being translated from maternal RNA stores. However, components of adherence junctions are not organized into junctional complexes until the 8-cell stage. Posttranslational modifications, such as phosphorylation, are thought to lead to the association of these proteins to form a functional complex and hence compaction (Kemler, 1993). Presumably, control of the process of assembly is regulated by the embryo itself after activation of the embryonic genome at the 2-cell stage. However, the factors involved in regulation of these processes are unknown.

Development of preimplantation embryos *in vitro* is density dependent, suggesting that diffusible factors secreted by the embryos support embryonic growth. Preimplantation embryos have been shown to express fibroblast growth factor 4 (FGF4; Rappolee *et al.*, 1994) and the high-affinity fibroblast growth factor receptors 1, 2, 3, and 4 (FGFR1, -2, -3, -4; Rappolee *et al.*, 1998; Haffner-Krausz *et al.*, 1999). Deletion of individual *Fgf* and individual *Fgfr* genes does not result in preimplantation lethality before the blastocyst stage, suggesting that expression of each individual one of these genes is not essential for the early phase of development. The earliest lethalities found in mutating members of the FGF signaling system occur around implantation (Feldman *et al.*, 1995; Arman *et al.*, 1998). Interestingly, the expression of a dominant negative FGFR in preimplantation mouse embryos causes zygotic cell division to cease at the fifth division (Chai *et al.*, 1998). This suggests that FGF signaling is required for preimplantation development, but may be a highly redundant system or may be reliant on maternal FGF4.

Relatively few genes are known to be necessary for development before the blastocyst stage, partly because essential processes are supported by proteins translated from maternal mRNA until this stage. Therefore, a severe phenotype prior to the blastocyst stage may indicate that the gene affected is required for the embryo to activate its own genome. Several mutations exist showing abnormal preimplantation development before the blastocyst stage. These include mdm (Cheng and Constantini, 1993), Om/DDK, oligosyndactyly, and the T-complex mutations t^{12} and tw^{32} (Magnuson and Epstein, 1981). However, in these mutations the affected genes have not been identified. Progress in understanding how preimplantation embryos establish regulation of transcription and their own pattern of gene expression from a completely inactive genome has been hampered by the lack of molecules known to regulate these processes.

In this paper we describe the isolation, characterization, and the loss-of-function phenotype of a previously undescribed mouse gene, *Traube (Trb)*, which is essential for preimplantation development. The majority of homozygous embryos develop normally until the compacted morula stage. Then most of the mutant embryos fail to form blastocysts, decompact, and die a day later. We hypothesize that TRB is important in establishing embryonic gene expression.

MATERIALS AND METHODS

Generation of the mutant Trb^{gt} allele. The promoterless reporter construct *pGT1.8geo* (kindly provided by W. Skarnes; Skarnes *et al.*, 1995) was electroporated into the parental murine ES cell line MPI-II (Voss *et al.*, 1997) as described previously (Voss *et al.*, 1998b).

Cloning and sequencing of the Trb cDNA. Total RNA was isolated from ES cells heterozygous for the insertion of *pGT1.8geo* into the murine genome (clone P66). 5′ rapid amplification of cDNA ends was performed as previously described (Voss *et al.*, 1998a) using oligonucleotides complementary to the *lacZ* gene of *pGT1.8geo* as gene-specific primers. RACE products were isolated and sequenced. The sequences specific for the endogenous gene were amplified by PCR, cloned into *pGemT* (probe 1, Fig. 1A), and used as a probe to screen an ES cell cDNA library. The ES cell cDNA library was generated for this purpose. Poly(A)$^+$ RNA from wild-type ES cells (MPI-II) was reverse-transcribed with random hexamere oligonucleotides and second-strand synthesis was carried out using a cDNA synthesis kit (Pharmacia). After filling-in reaction, ligation to *Eco*RI/*Not*I adapters (Pharmacia), and size selection on a Sephacryl S-400HR column, the cDNA was cloned into the *Eco*RI site of λ*pExcell* (Pharmacia) and packaged into Gigapack III Gold (Stratagene). *Escherichia coli* NM522 were transfected with the phages and plated. The cDNA library of 1,000,000 plaques was harvested without further amplification. The average insert size was 2 kb ± 0.8; β-actin was represented with 0.17%. With clones isolated from this library a poly(dT)-primed Postnatal Day 20 brain cDNA library (Stratagene) was screened.

Sequence comparison. The deduced protein sequence was encoded by the longest open-reading frame, started with the first start codon, and was in frame with the *lacZ* ORF. The cDNA sequence and the protein were compared to entries into the EMBL, SwissProt, and GenBank data base by fasta analysis (Wisconsin Package, Genetics Computer Group, Inc.). Similarities between TRB and TRB-related proteins were analyzed using ClustallW (Thompson *et al.*, 1994) and MacBoxshade (http://www.ch.embnet.org/software/BOX_form.html).

Generation of the mutant Trb^{gt} mouse line. Chimeras were produced by a technique modified from Nagy and Rossant (1993) omitting the sandwich technique (Voss *et al.*, 1998b). Chimeras were mated to wild-type females of the mouse strains C57Bl/6 and

NMRI to produce animals heterozygous for the Trb^{gt} mutation. In time-pregnant female mice, noon of the day on which the vaginal plug was observed was termed Day 0.5 of gestation (E0.5). Mice were genotyped by quantitative Southern using a neomycin phosphotransferase probe and a control probe as described previously (Thomas *et al.*, 1998).

Whole embryo and histological analysis. Embryos were flushed from their mothers' uteri, placed in M2, and viewed and photographed using an inverted microscope (Labovert, Leitz) or a differential interference contrast optic microscope (Axiophot 2, Zeiss). For histological analysis embryos were fixed in 2.5% glutaraldehyde and, with intervening PBS washes, postfixed in 1% osmium tetroxide, dehydrated, infiltrated, and embedded in Epon. Five-hundred-nanometer sections were cut and stained with stained toluidine blue. Eighty-nanometer sections were stained with 1% uranyl acetate and 1% lead citrate and used for transmission electron microscopy.

Northern analysis, in situ hybridization, and β-galactosidase staining. Northern blots were prepared by standard techniques and hybridized with a [α-^{32}P]dCTP labeled the *Trb*-specific probe 1 described above (Fig. 1A). Filters were autoradiographed for 14 days. *In situ* hybridization was performed essentially as described (Hogan *et al.*, 1994). Briefly, section were deparaffinized, rehydrated, incubated for 10 min (or 30 min for adult brains) at room temperature in 10 mg/ml proteinase K, fixed in 4% paraformaldehyde for 10 min, and then dehydrated. Sections were air-dried, and then hybridization solution containing 5×10^5 cpm/μl *in vitro* transcribed cRNA probe (probe 2, Fig. 1A) was placed onto the section. Slides were incubated overnight at 56°C and then washed as described (Hogan *et al.*, 1994). Slides were autoradiographed at 4°C for 14 days, developed, and counterstained with hematoxylin. Embryos were stained for β-galactosidase activity as described previously (Thomas *et al.*, 1998). For staining of preimplantation embryos 0.1% BSA was added to all solutions except the staining solution to reduce stickiness and embryos were fixed for 3 min only.

Myc tagging. The coding sequence of the *Trb* cDNA was cloned in frame with 5 myc epitopes (Roth *et al.*, 1991) into *pCS2 + MT* and sequenced to confirm the successful cloning. The tagged protein was *in vitro* translated. The *Trb/5myc*-containing plasmid was transfected into COS7 or NIH3T3 cells using Lipofectamine (Gibco BRL). Twenty-four hours after the transfection the cells were fixed in 4% paraformaldehyde, subjected to myc immunofluorescence detection using a mouse monoclonal anti-c-myc (9E10, Santa Cruz, 1:100) and an Alexa 568 goat anti-mouse antibody (Molecular Probes, 1:500), and counterstained with DAPI.

Embryo culture. Embryos of $Trb^{gt/+}$ heterozygous mutant intercrosses were isolated and cultured in M16 under oil. Control cultures were established with embryos wild type at the *Trb* locus.

Generation and processing of chimeric embryos. For chimeric analysis of the mutant phenotype *in vitro*, embryos of $Trb^{gt/+}$ heterozygous mutant intercrosses were recovered in the 8-cell stage, labeled with a lipophilic fluorescent dye (CellTracker CM-DiI, Molecular Probes), and aggregated with wild-type unlabeled embryos, essentially as describe previously (Nagy and Rossant, 1993). As controls, embryos wild type at the *Trb* locus were labeled and aggregated with unlabeled wild-type embryos. The aggregates were cultured for 24 h in M16 under oil and then viewed and photographed with a fluorescent microscope (Axiophot 2, Zeiss).

Immunocytochemistry and β-actin staining. Zonae pellucidae were removed from preimplantation unhatched embryos with acid Tyrode's solution. Embryos were fixed in 2% paraformaldehyde in PBS and incubated with intervening and a final incubation in PBS plus 0.25% gelatine in 0.1% Triton X-100 in PBS, first antibody solution, and second, fluorescent antibody solution. One PBS plus gelatine wash solution also contained 0.1 μg/ml of the fluorescent nuclear stain Hoechst 33258 (Molecular Probes). Then they were mounted with an aqueous mounting medium (Mowiol) and viewed and photographed using a fluorescence microscope (Axiophot 2, Zeiss). The first antibodies and dilutions used were goat anti-human α-E-catenin (Santa Cruz, 1:50), mouse monoclonal anti-mouse β-catenin (Transduction Laboratories, 1:50), mouse monoclonal anti-human E-cadherin (Transduction Laboratories, 1:2500), goat anti-human occludin (Santa Cruz, 1:50), goat anti-human ZO1 (Santa Cruz, 1:20), goat anti-human FGF4 (Santa Cruz, 1:50), rabbit anti-human FGFR1 (anti-Flg, Santa Cruz, 1:100), mouse monoclonal anti-human FGFR2 (anti-Bek, Santa Cruz, 1:20), rabbit anti-human FGFR3 (Santa Cruz, 1:100), and goat anti-mouse FGFR4 (Santa Cruz, 1:50). The part of the human proteins that were used as antigens was identical between human and mouse except for E-cadherin and FGFR3. The occludin peptide differed by two amino acids. The anti-FGFR2 antibody was raised against a carboxy-terminal peptide and, therefore, recognizes both the IIIb and IIIc splice variant. The second antibodies used were Alexa 568 donkey anti-goat IgG, Alexa 568 goat anti-mouse IgG, and Alexa 568 goat anti-rabbit IgG (all Molecular Probes, 1:1000). In our hands FGFR2 was detectable in inner cell mass cells and trophectoderm cells at E3.5. In contrast, Haffner-Krausz and co-workers reported trophectoderm restriction of this receptor (Haffner-Krausz *et al.*, 1999).

TUNEL and trypan blue exclusion test. The zonae pellucidae were removed from E3.5 embryos recovered from $Trb^{gt/+}$ heterozygous mutant intercrosses or wild-type intercrosses. The embryos were fixed for 10 min in 1% paraformaldehyde in PBS, washed in PBS, and dried onto object slides. On the slides they were processed with intervening PBS washes through 0.1% Triton X-100 for 15 min, equilibration buffer, terminal transferase reaction incorporating digoxigenin-labeled deoxynucleotide, fluorescein-labeled anti-digoxigenin antibody (all ApoTag *in situ* apoptosis detection kit, Oncor Appligene). As positive controls, embryos were treated with 0.5 μg/ml Dnase I after the permeabilization step. The slides were covered with an aqueous mounting medium (Mowiol) to which 0.5 μg/ml Hoechst 33258 was added. The embryos were viewed and photographed using a fluorescence microscope (Axiophot 2, Zeiss). For trypan blue exclusion embryos were recovered and incubated for 10 min in 0.4% trypan blue in M16 culture medium, washed in M2, and then viewed immediately under an inverted microscope (Labovert, Leitz). As positive controls wild-type embryos were killed using sodium azide.

Statistics. Total cell number and rate of apoptosis and mitosis of wild-type and homozygous $Trb^{gt/gt}$ embryos were compared by Student's *t* test. Means are given ± standard deviation.

RESULTS

Isolation and Cloning of the Traube cDNA and Generation of the Mutant Allele

In a gene trap screen for genes important in embryonic development (Voss *et al.*, 1998b) we isolated a previously undescribed murine gene which we called *Traube* (*Trb*, grape). RACE products of up to 200 bases were isolated and sequenced. The sequences specific for the endogenous gene were cloned into *Bluescript KS+* (Stratagene; probe 1, Fig. 1A) and used as a probe to screen a random-primed ES cell

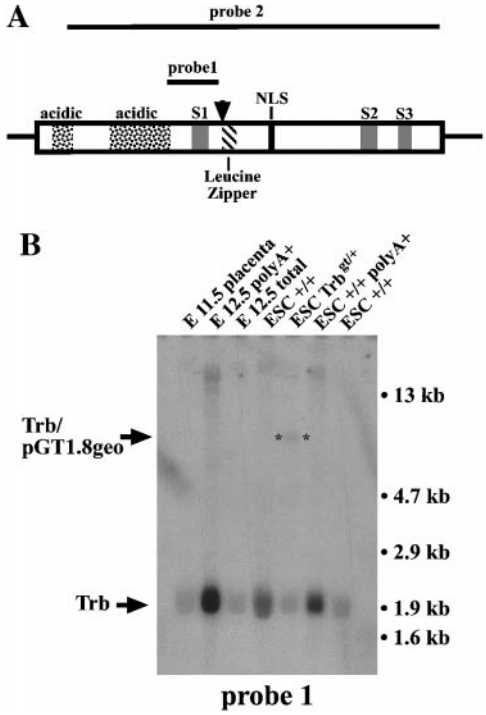

FIG. 1. Structure of *Trb* mRNA. (A) Schematic drawing of the *Trb* mRNA sequences coding for two acidic domains (checked, aa 21 to 49 and aa 94 to 173), a leucine zipper (striped, aa 242–263), three putative nuclear localization signals (NLS, black, aa 304–311), and the position of the gene trap insertion at base 853 (arrowhead) are indicated. Gray boxes indicate sequences coding for three areas of particular sequence similarity to TRB-related proteins (S1, S2, S3, also see Fig. 2) between aa 208 and aa 222, aa 424 and aa 443, and aa 466 and aa 485. (B) Northern analysis of total RNA of E11.5 placenta, poly(A)$^+$ RNA and total RNA of E12.5 embryo, total RNA of wild-type ES cell and ES cells heterozygous for the gene trap insertion at the *Trb* locus, and poly(A)$^+$ and total RNA of wild-type ES cells probed with a *Trb*-specific probe (probe 1 in A). The positions of the 16S (1.6 kb), 18S (1.9 kb), 23S (2.9 kb), 28S (4.7 kb), 45S (13 kb) ribosomal RNA of *E. coli* and mouse used as molecular weight markers, the *Trb* mRNA, and the *Trb*/pGT1.8geo fusion mRNA are indicated. The position of the fusion mRNA is marked with asterisks.

cDNA library made for this purpose. Overlapping cDNA clones isolated from this library coded for bases 1 to 1693. The remaining 3′ untranslated region (UTR) was obtained by screening a poly(dT)-primed Postnatal Day 20 brain cDNA library. The two clones isolated from this library contained almost the entire sequence previously produced by screening the ES cell library confirming that these represented transcripts of the same gene. The *Trb* mRNA was 1.9 kb in length, as shown by Northern analysis (Fig. 1, submitted to the EMBL data base, Accession No. F222801). Since this mRNA is of a similar size to the 18S ribosomal RNA and expressed only at low levels, we confirmed that this is the true length of the *Trb* mRNA by comparing the signal from Northern analysis of Poly(A)$^+$ RNA and total RNA (Fig. 1B). The 5′ UTR was 119 bases and the 3′ UTR 100 bases long. The putative open-reading frame of 1581 bases started at the first ATG which was a non-Kozak sequence (Kozak, 1989). This open-reading frame coded for a protein of 526 amino acids. The deduced protein contained a putative leucine zipper with perfect leucine spacing and predicted coiled coil secondary structure between aa 242 and aa 263 (predicted as described by Bornberg-Bauer *et al.*, 1998). Two acidic domains were found at aa 21 to 49 and at aa 94 to 173 which were high in glutamic acid content. Furthermore, three putative nuclear localization signals were found, one 4 residue pattern at aa 305, and two 7 residue patterns at aa 304 and 305 (NLS, Psort II, proteomics tools, SwissProt).

The gene trap insertion occurred at base 853 with respect to the cDNA and deleted the last 281 of 526 amino acids. The use of the splice acceptor and polyadenylation signal of the gene trap construct resulted in a protein truncated at aa 245, amino-terminal of the leucine zipper and fused to a β-galactosidase/neomycin phosphotransferase fusion protein. This fusion protein lacked the leucine zipper and the putative nuclear localization signals, but retained the acidic domains. As there was no transport of the fusion protein into the nucleus (see below), we concluded that this fusion protein did not retain any functional activity and was unlikely to have any dominant negative effects. The heterozygous animals developed and lived normally indicating that fusion protein generated from one mutant allele had no adverse effect. The fusion protein containing the first 245 aa of TRB we called TRB245/β-gal/neo.

TRB-Related Proteins

Searches through the EMBL, GenBank, and SwissProt gene and protein data bases yielded two unpublished human cDNAs, *Che1* (Accession No. AF083208) and *Ded* (Accession No. AJ249940), rat *AATF* (Accession No. AJ238717; Page *et al.*, 2000), and an unpublished protein sequence of *S. cerevisiae* (Accession No. Q06631, Fig. 2). The TRB protein showed 95% sequence similarity to the rat protein, suggesting that AATF may be the rat homologue of TRB. TRB exhibited 75% sequence similarity to the human protein CHE1 and 31% to the yeast protein. TRB and the human proteins CHE1 and DED exhibited a high degree of similarity and identity. *Che1* and *Ded* may actually be the same gene. Both show an identical degree of identity and similarity to a clone of human chromosome 17 (Accession No. AC003103). The area of human chromosome 17 (17q12–q21) where *Che1* and *Ded* are localized corresponds to mouse chromosome 11 (58–63 cM). Three regions of particular sequence similarity among TRB, the rat, the human, and the yeast protein, were found in amino acids 208 to 222, 424 to 443, and 466 to 485 of the TRB sequence (i.e., at aa 241 to 255, 459 to 478, and 502 to 521 of the sequence comparison in Fig. 2). In these regions of sequence similarities TRB and the TRB-related proteins are predicted

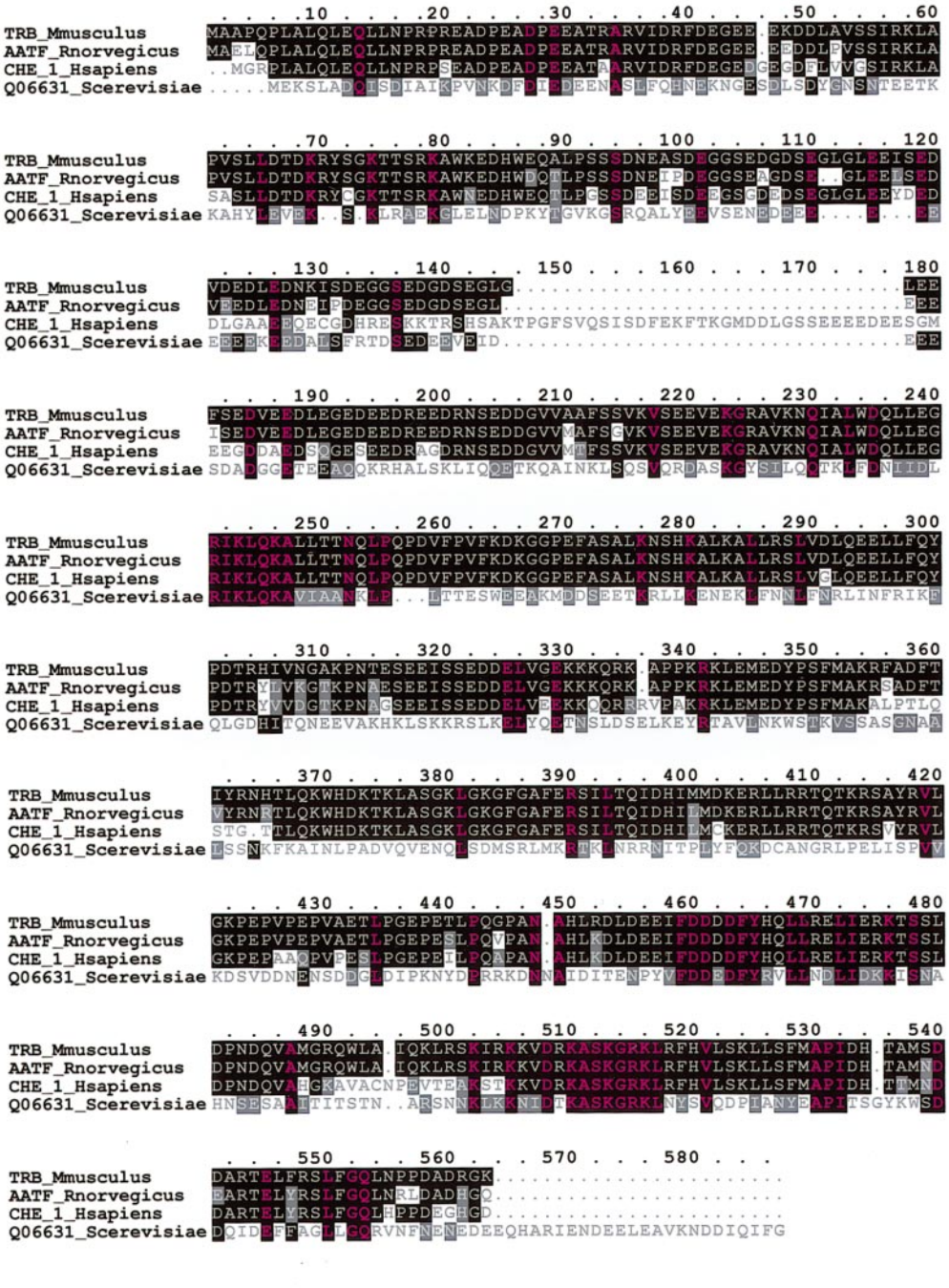

	mouse	rat	human	yeast
TRB_Mmusculus	----	94.9	75.0	30.7
AATF_Rnorvegicus	92.6	----	75.0	30.5
CHE_1_Hsapiens	72.9	73.4	----	27.0
Q06631_Scerevisiae	18.4	18.0	15.2	----

FIG. 2. Sequences comparison of TRB and related proteins. Amino acid sequence comparison of the deduced TRB protein (TRB_M.musculus), AATF of *R. norvegicus* (Accession No. AJ238717; Page *et al.*, 2000), an unpublished protein of *H. sapiens* (Che1, Accession No. AF083208), and an unpublished protein of *S. cerevisiae* (Accession No. Q06631). Identical amino acid residues are shown shaded black with those amino acids present in all sequences in red, similar residues are shaded gray, and different residues are not shaded. The percentage of sequence identity is shown in the lower half, and the percentage of sequence similarity in the upper half of the table inserted. Note that

to form helical and coil structures (King and Sternberg, 1996).

Expression Pattern of Trb

Northern analysis showed that *Trb* was detectable at very low levels in midgestation embryos, fetal placentae, and ES cells. The Northern blot autoradiogram shown in Fig. 1B was exposed for 2 weeks and clearly visible bands were present only in lanes loaded with poly(A)$^+$ RNA. Insertion of the gene trap construct resulted in the production of a fusion mRNA between the 853 bases of endogenous RNA and about 4.5 kb of the lacZ and neomycin phosphotransferase sequences of pGT1.8geo. The fusion mRNA was of the expected size of about 5.4 kb (Fig. 1B). Comparison of the β-galactosidase activity pattern of the fusion protein and radioactive *in situ* hybridization using a *Trb*-specific probe showed that the reporter reflected the activity of the endogenous locus faithfully (compare Figs. 3D and E, and Figs. 4A and C). β-Galactosidase activity was first observed in all cells of preimplantation embryos at E2.5 and in E3.5 embryos (E3.5 shown in Fig. 3A). Likewise, at E6.5 *Trb* is expressed in all cells (Fig. 3B). At E7.5 and E8.5 β-galactosidase activity and *Trb* expression were observed in all cells of the embryo proper, and stronger expression was seen in the extraembryonic ectoderm (Figs. 3D, E, G, and H). The *Trb* gene was expressed relatively uniformly in all cells of the embryos until E10.5. At E11.5 stronger β-galactosidase activity and *Trb* expression were observed in the liver, the posterior commissure, the hind brain, the spinal cord, and the dorsal root ganglia (Figs. 4A and C). *In situ* hybridization showed that at E12.5 *Trb* expression in the liver was restricted to the hepatocytes, whereas the hematopoietic cells did not express *Trb* (Fig. 4E). At E15.5 *Trb* was expressed in the nervous system in the mammallary bodies, the medulla, and the spinal cord (Fig. 4F) and in the liver (not shown). In adult brain *Trb* expression was restricted to the Purkinje cells of the cerebellum (Fig. 4G).

TRB Is a Nuclear Protein

A myc-tagged TRB protein was expressed in COS7 cells and NIH3T3 cells and subjected to myc-specific immunofluorescence labeling. The TRB/5MYC fusion protein was localized to the nuclei of both cell types (COS7 cells shown in Figs. 5A, C, and E), whereas the 5 MYC epitopes expressed alone were evenly distributed to all cell compartments (not shown). In about half the cells the TRB/5MYC protein was localized to the nucleoli (Fig. 5) which are stained less intensely with Hoechst 33258 than other areas of the nucleus. The TRB245/β-gal/neo fusion protein generated from the mutant Trb^{gt} locus was expressed in $Trb^{gt/+}$ ES cells. The gene trap insertion truncated the endogenous protein and, thereby, caused loss of the putative nuclear signals. Accordingly, β-galactosidase activity was found in the cytoplasm supporting the hypothesis that the putative localization signals were utilized for nuclear translocation.

The $Trb^{gt/gt}$ Mutant Phenotype in Vivo

Animals heterozygous for the Trb^{gt} mutant allele were viable and morphologically indistinguishable from wild-type controls. Female and male heterozygotes transmitted the mutant allele through their germ line in a 1:1 ratio (n = 50, each for male and female), indicating that the Trb^{gt} oocytes and spermatocytes developed normally and underwent normal fertilization and cleavage divisions. We did not recover $Trb^{gt/gt}$ homozygous animals or embryos among a total of 151 offspring of $Trb^{gt/+}$ heterozygous intercrosses at 3 weeks of age, E15.5, E12.5, E9.5, E8.5, or E7.5. Instead, we found wild-type and heterozygous animals in a ratio of 1:2 (Table 1). We did not observe resorbed implantation sites at the embryonic stages. One-quarter of the embryos recovered at E3.5 showed twice the intensity of β-galactosidase staining as heterozygous embryos (n = 43), indicating that homozygous embryos were present at this stage of development. At E2.5 all embryos recovered from $Trb^{gt/+}$ heterozygous intercrosses were morphologically normal compacting morulae (Fig. 6A). At E3.5 those embryos staining stronger for β-galactosidase activity exhibited an abnormal morphology. Of 316 embryos recovered from $Trb^{gt/+}$ heterozygous intercrosses at E3.5, 243 (77.5%) exhibited the normal morphology of blastocysts (Table 2 and Figs. 6B and D). In contrast, 73 (22.5%) showed abnormal morphology (Figs. 6C and E). Most of the abnormal embryos (88%) had not formed a blastocoel cavity. Although the majority of the cells in these abnormal embryos were compacted, individual blastomeres were not compacted. The uncompacted cells were rounded and had minimal content areas to the neighboring cells (Fig. 6C vs A and B, and E vs D). A few mutant embryos (12%) developed into small abnormal blastocysts which consisted of only a few cells and also exhibited individual uncompacted cells. Compacted and uncompacted cells of the mutant E3.5 embryos generally excluded the vital dye trypan blue showing that the cell membranes were still intact at this point. E3.5 embryos recovered from matings of either a male or a

---

the human, the mouse, and the rat sequence are highly conserved and that the yeast sequence shows three areas of particularly high degree of similarity to the other three at aa 241 to 255, 459 to 478, and 502 to 521 in this sequence compilation (corresponding to aa 208 to 222, 424 to 443, and 466 to 485 of the TRB sequence, respectively). In this comparison the position of the leucine zipper is between aa 275 and aa 297 and is conserved between mammalian species but is not found in the yeast protein. The NLS at aa 338–345 is likewise not found in a conserved position in yeast.

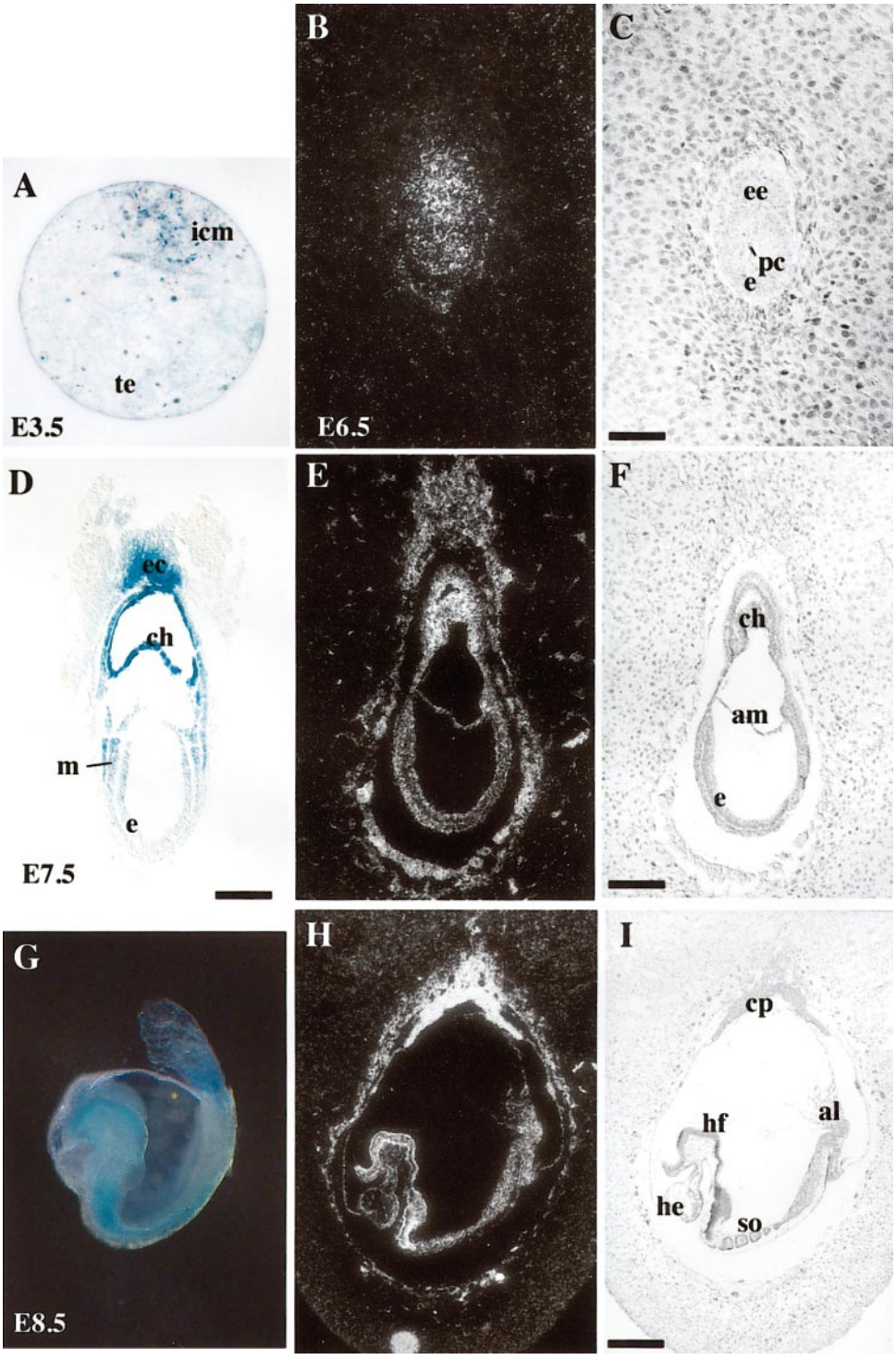

FIG. 3. Expression pattern of *Trb* from E3.5 to E8.5. Embryos recovered from matings involving 1 or 2 $Trb^{gt/+}$ heterozygous parents stained for activity of the β-galactosidase reporter (A, D, G) or paraffin sections of wild-type embryos hybridized *in situ* with a *Trb*-specific cRNA probe (probe 2 in Fig. 1A). Dark-field images (B, E, H) and corresponding bright-field images (C, F, I). (A) E3.5 embryo, (B, C) E6.5, (D, E, F) E7.5, (G, H, I) E8.5. Note ubiquitous expression of the *Trb* gene at these stages of development with slightly higher expression in the inner cell mass at E3.5 and the extraembryonic ectoderm at E7.5 and E8.5. Al is allantois; am, amnion; ch, chorion; cp, chorionic plate; e, embryonic ectoderm; ec, ectoplacental cone; ee, extraembryonic ectoderm; he, heart; hf, head fold; icm, inner cell mass; m, mesoderm; pc, proamniotic cavity; so, somites; te, trophectoderm. Bars are 27 μm in A; 84 μm in B and C; 175 μm in D, E, and F; and 350 μm in G, H, and I.

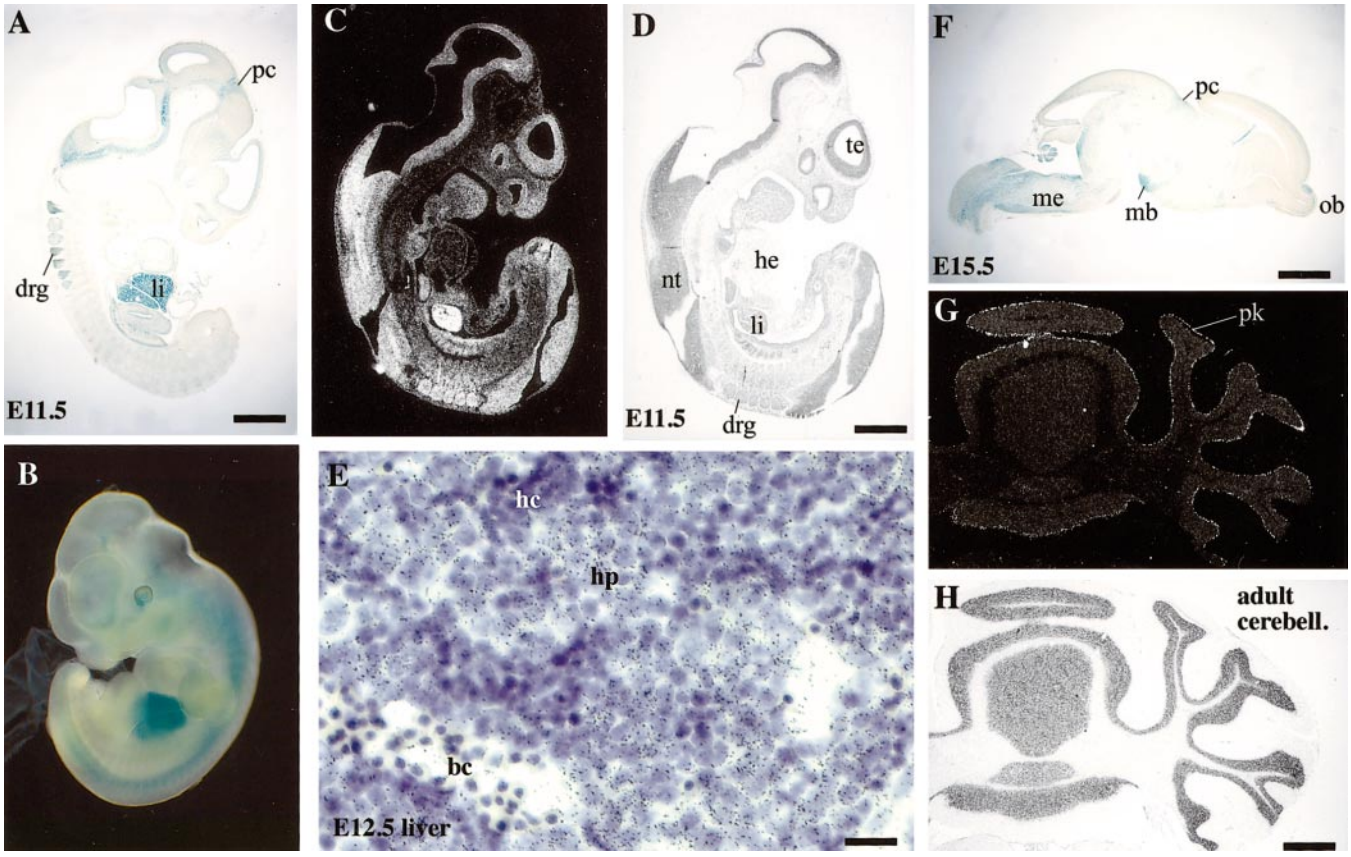

FIG. 4. Expression pattern of *Trb* at E11.5, in E12.5 liver, E15.5, and adult brain. Embryos or tissues recovered from matings involving 1 or 2 $Trb^{gt/+}$ heterozygous parents stained for activity of the β-galactosidase reporter (A, B, F) or paraffin sections of wild-type embryos or tissues hybridized *in situ* with a *Trb*-specific cRNA probe (probe 2 in Fig. 1A). Dark-field images (C, G), corresponding bright-field images (D, H), and bright-field image (E). (A, B, C, D) E11.5 embryo, (E) E12.5 liver, (F) E15.5 brain, (G, H) adult cerebellum. Note that compared to earlier stages, at E11.5 expression of *Trb* was modulated. Low level expression was observed in many tissues, but high expression was restricted to the liver and the nervous system, namely the posterior commissure, the hindbrain, the spinal cord, and the dorsal root ganglia. Expression of *Trb* in the liver was restricted to the hepatocytes. At E15.5 expression was prominent in the mammallary bodies, and the medulla. In adult brain *Trb* expression was restricted to the Purkinje cells of the cerebellum. Bc are blood cells; drg, dorsal root ganglia; hc, hematopoietic cells; he, heart; hp, hepatocytes; li, liver; me, medulla; mb, mammillary bodies; nt, neural tube; ob, olfactory bulb; pc, posterior commissure; pk, Purkinje cells. Bars are 560 μm in A, B, C, and D; 15 μm in E; 900 μm in F; and 640 μm in G and H.

female $Trb^{gt/+}$ heterozygous animal to wild-type mice were all normal blastocysts.

The $Trb^{gt/gt}$ Mutant Phenotype in Vitro

All 36 embryos recovered from $Trb^{gt/+}$ heterozygous intercrosses at E1.5 were normal 2-cell stage embryos. They were cultured in M16 under oil. Within 24 h they all developed to normal compacting or compacted morulae. After 48 h of culture 27 (75%) developed to blastocysts with normal morphology. The remaining 9 (25%) did not form blastocysts (Table 2). Instead, they had started to decompact. While the majority of the cells were still compacted, some of the blastomeres had been extruded from these embryos which had been compacted 1 day earlier. After 72 h of culture these abnormal embryos had died and disintegrated within their zona pellucida, whereas the other 75% were fully expanded blastocysts, most of which had hatched from their zona pellucida. In control cultures 100% of the embryos developed to blastocysts.

From the observations *in vivo* and *in vitro* we concluded that $Trb^{gt/gt}$ mutant homozygous embryos generally did not develop beyond the compacted morula stage. In exceptional cases, they did form small abnormal blastocysts. Mutant embryos did not hatch from their zonae pellucidae and did not cause a decidual reaction.

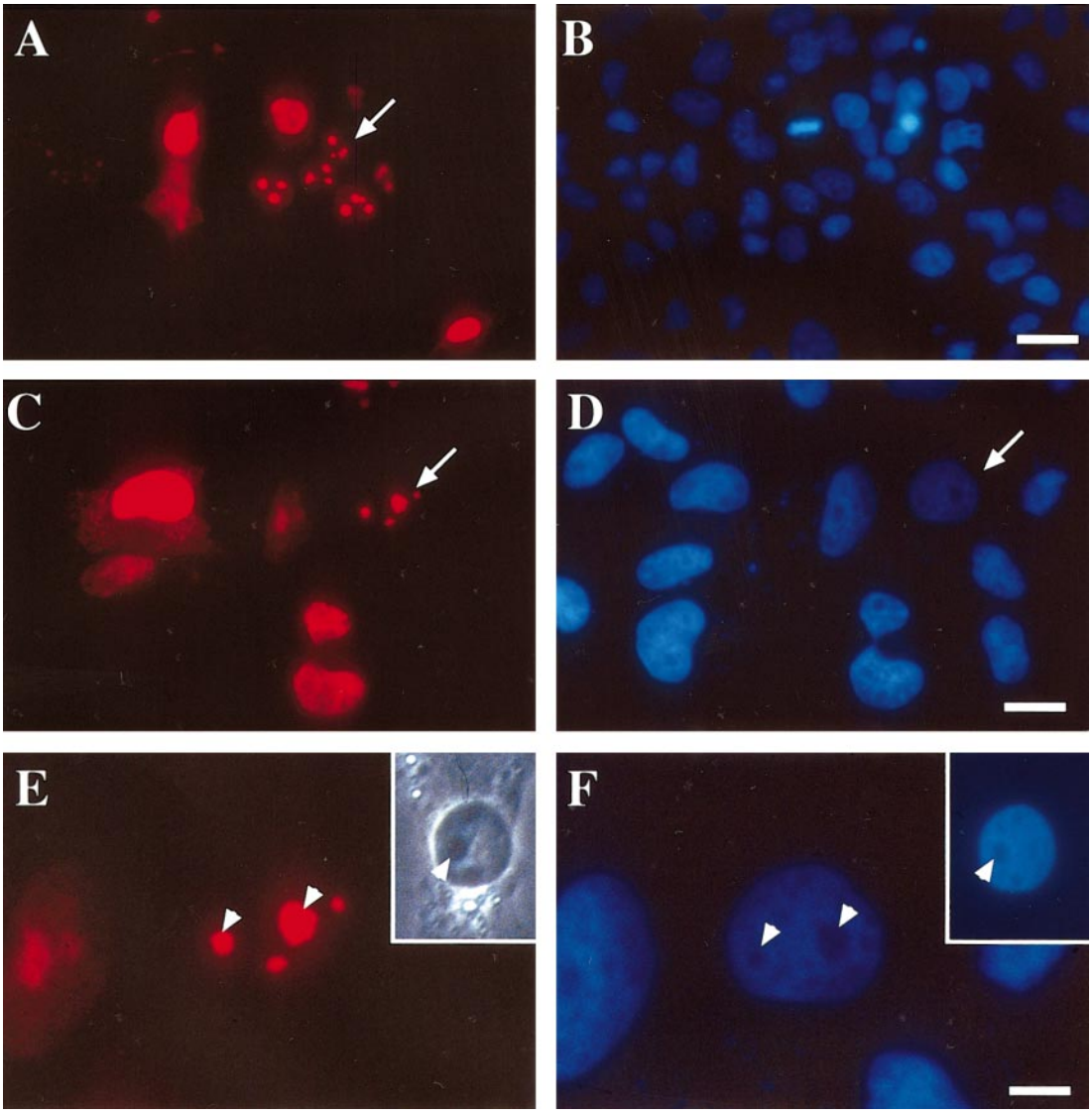

FIG. 5. Subcellular localization of TRB protein. MYC immunocytochemistry of COS7 cells transfected with a construct coding for a TRB/5MYC fusion protein. (A, C, E) MYC immunofluorescence, (B, D, F) nuclear stain DAPI. Note the localization of the MYC immunofluorescence to the nuclei and specifically to the nucleoli (arrows in A, C, D, and arrowheads in E and F). Insert in E shows phase contrast of the DAPI-stained nucleus inserted in F. Bars are 26 μm in A and B; 15 μm in C and D; and 7 μm in E and F.

Chimeric Analysis of the Trb Mutant Phenotype

In order to investigate if the *Trb*^{gt} mutation could be modified by the presence of wild-type cells, we recovered E2.5 embryos from *Trb*$^{gt/+}$ heterozygous intercrosses, labeled them with the lipophilic fluorescent dye, DiI (n = 59), aggregated them with unlabeled wild-type embryos, and cultured them *in vitro* for 24 h (Fig. 7A). As controls, embryos wild type at the *Trb* locus were labeled and aggregated with wild-type embryos. Of the mutant/wild-type aggregates 78% resulted in chimeric embryos that formed normal blastocysts (Figs. 7B and C). The remaining 22% failed to aggregate. In these cases the unlabeled wild-type embryos formed blastocysts. In contrast, the labeled aggregation partners did not form blastocysts and, instead, exhibited the mutant morphology (Figs. 7D and E). In control aggregations (n = 87) 98% of the aggregates formed chimeric blastocysts. The remaining 2% failed to aggregate, but the labeled and the unlabeled aggregation partners formed blastocysts. From these results we concluded that the *Trb*^{gt} mutation caused a cell-autonomous incapability to develop beyond the compacted morula stage.

TABLE 1

Distribution of the Trb^{gt} Allele among Offspring of Heterozygous Intercrosses

Age	+/+	L/+	L/L	Total
Weaning	35	66	0	101
E 15.5	2	7	0	9
E 12.5	3	5	0	8
E 9.5	0	10	0	10
E8.5[a]	6	8	0	14
E7.5[a]	3	6	0	9
Sum ≥ E 7.5	49 (32%)	102 (68%)	0	151 (100%)
E 3.5[a]	9	21	13	43

[a] Genotyping by lacZ staining, otherwise by Southern analysis.

Proteins of Cells Adhesion Complexes Were Present in Trb Mutant Embryos

We investigated the possibility that cell adhesion complexes were disturbed in *Trb*$^{gt/gt}$ mutant embryo, because proteins of cell adhesion complexes, namely E-cadherin and α-E-catenin, had been shown to be essential for the formation of blastocoel cavities and the maintenance of compaction (Larue *et al.*, 1994; Riethmacher *et al.*, 1995; Torres *et al.*, 1997). By immunofluorescence staining ($n \geq 30$ for each antigen) we observed comparable levels of α-E-catenin (Fig. 8D vs C), β-catenin (Fig. 8F vs E), and E-cadherin (Fig. 8H vs G) in mutant and control embryos. The β-actin filament staining with phalloidin was comparable in intensity in mutant and control embryos. But its diffuse distribution throughout the cell resembled the staining pattern we found in compacted morulae rather than the staining pattern we observed in blastocysts (Fig. 8B vs A). Likewise, the α-E-catenin, β-catenin, and E-cadherin appeared to be less stringently localized to the cell membranes in the mutants compared to the controls. From these results we concluded that these proteins necessary for the formation of adhesion complexes and the maintenance of blastocoel cavities were present at similar levels in mutant and control embryos. However, it appeared that the organization of the protein components to form functional adhesion complexes may have been less efficient in the mutants than in controls.

Tight Junctional Proteins Were Present in Trb Mutant Embryos

We also explored the possibility that an inefficiency to form tight junctions may play a role in the formation of the *Trb*$^{gt/gt}$ mutant phenotype. The tight junctional proteins occludin (Fig. 9B vs A) and zona occludens protein 1 (ZO1, Fig. 9D vs C) were present at comparable levels in mutants and controls. However, as in the case of the adhesion complex proteins the localization of occludin to the cell membrane was less pronounced. We concluded from this that, in principle, these tight junctional proteins were present, although the formation of tight junctions did not develop beyond the stage typical of E2.5 embryos.

Gap Junctions Were Established in Trb Mutant Embryos

We performed cytoplasmic microinjection of a fluorescent dye, lucifer yellow, as a functional test of gap junctions, because previous reports described phenotypic abnormalities similar to those seen in the *Trb*$^{gt/gt}$ mutants when the formation of gap junctions was blocked by injection of antibodies against gap junctional proteins (Lee *et al.*, 1987). One cell each of embryos recovered from *Trb*$^{gt/+}$ heterozygous intercrosses at E2.5 or E3.5 ($n = 43$) and control embryos was injected with lucifer yellow. Dye injection into one cell of a normal compacted morula resulted in the rapid distribution of the dye to all cells of the embryo within 2 min (Fig. 9E). After injection into a blastomere of a normal 8-cell stage embryo the dye was not, or not appreciably, transported to the other blastomeres even after 30 min (Fig. 9F). The dye was rapidly distributed in normal E3.5 blastocysts (Fig. 9I). After injection into mutant embryos lucifer yellow was distributed among those cells that maintained compaction. In contrast, the dye was not transported to those cells that had been extruded (Fig. 9J). From this we concluded that gap junctions formed in mutant embryos, but were not maintained when decompaction occurred.

FGF4 and the FGFR1, -2, -3, and -4 Were Present in Trb Mutant Embryos

The fact that the expression of a dominant negative fibroblast growth factor receptor resulted in phenotypic abnormalities (Chai *et al.*, 1998) similar to those seen in our *Trb*$^{gt/gt}$ mutant embryos prompted us to investigate if the fibroblast growth factor shown to be important in early embryonic development, namely FGF4 (Feldman *et al.*, 1995), and the high-affinity FGF receptors 1, 2, 3, and 4 were expressed normally in embryos from *Trb*$^{gt/+}$ heterozygous intercrosses at E3.5. We found that all of these proteins were expressed in the mutant embryos (Fig. 10) and transported into the nucleus where appropriate (Johnston *et al.*, 1995). We concluded from this that it was unlikely that the *Trb*$^{gt/gt}$ mutant phenotype was caused by a defect in FGF4 signaling.

Trb Mutant Embryos Showed a Severe Reduction in Cell Proliferation before Blastocyst Formation

We employed the fluorescent DNA stain Hoechst 33258 to stain the nuclei of 269 embryos recovered from *Trb*$^{gt/+}$ heterozygous intercrosses at E3.5. The total number of cells, the number of mitoses, and the number of cell undergoing cell death involving chromatin condensation and fragmentation were counted per embryo. The total number of cells was reduced by half in the mutant embryos

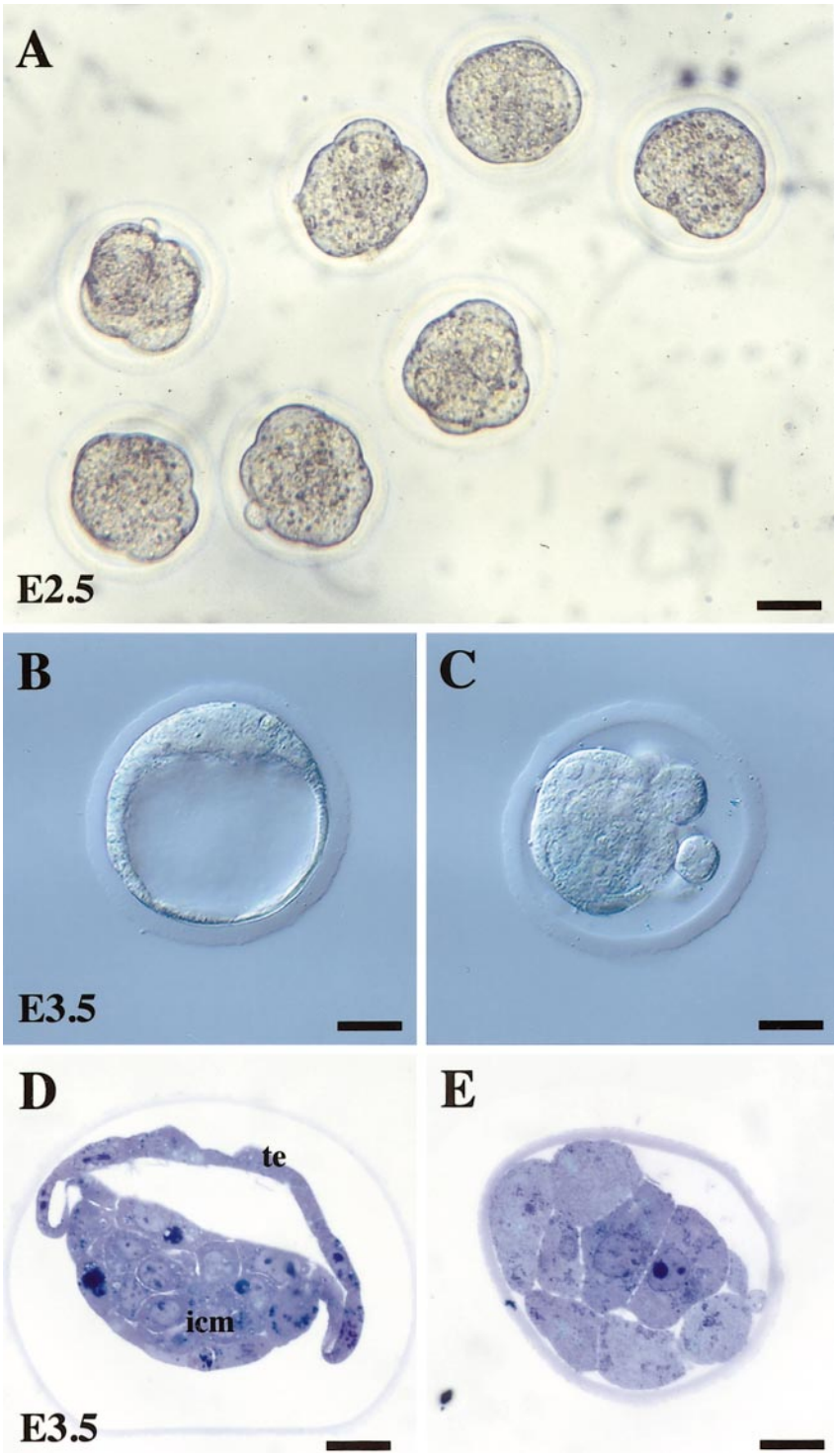

FIG. 6. Phenotype of $Trb^{gt/gt}$ mutant embryos. (A) E2.5 embryos recovered from $Trb^{gt/+}$ heterozygous intercrosses; (B, C) control and mutant morphology, respectively, at E3.5 photographed with differential interference contrast optics, (D, E) 500-nm Epon sections stained with toluidine blue showing control and mutant morphology, respectively, at E3.5. The control embryo in D partially collapsed during the embedding process. Note the extrusion of individual blastomeres in C and E from mutant embryos which previously were compacted as shown in A. Also note the small number of large blastomeres in the mutant morphology (E) indicating that the efficiency of cell division is greatly reduced before E3.5. Icm is inner cell mass; te is trophectoderm. Bars are 36 μm in A; 23 μm in B and C; and 19 μm in D and E.

TABLE 2

Developmental Capacity of $Trb^{gt/+}$ × $Trb^{gt/+}$ Embryos *in Vivo* and *in Vitro*

Experiment	Normal morphology	Abnormal[a] morphology	Total number of embryos
Embryos recovered E3.5	243 (77.5%)	73 (22.5%)	316 (100%)
Embryos recovered E1.5	36 (100%)	0	36 (100%)
Cultured for 1 day	36 (100%)	0	36 (100%)
Cultured for 2 days	27 (75%)	9 (25%)	36 (100%)

[a] In most cases blastocoel cavities had not formed and blastomeres were extruded from morulae.

(23 ± 6.2 vs 48 ± 11.6, $P \leq 0.05$; Fig. 11A vs B, and E). In contrast, the total number of cells undergoing mitosis or cell death per embryo as well as the rates of apoptosis and mitosis were not significantly different between mutants and controls. In fact, the cell size of the blastomeres was much larger in the mutants than in the controls (Fig. 6E vs D) similar to the cell size in compacted morulae. This also indicated that a deficiency in cell division rather than an increase in cell death accounted for the lower cell number. Terminal deoxynucleotide transferase-mediated dUTP-digoxigenin nick-end labeling (TUNEL) stained those cells which, using the nuclear stain Hoechst 33258, showed cell death involving chromatin condensation ($n = 58$, Figs. 11C and D).

From these results we concluded that TRB was crucial for efficient cell division from the compacted morulae stage onward.

Electron Microscopy

E3.5 embryos of $Trb^{gt/+}$ heterozygous intercrosses were processed for transmission electron microscopy. Mutant embryos (Figs. 12B and C) showed a paucity of ribosomes, polyribosomes, and rough endoplasmic reticulum as compared to controls (Fig. 12A) or even as compared to compacted morulae. The external appearance of the embryo in B showed it to be at an earlier stage of mutant phenotype pathogenesis than the embryo in C. Cortical filaments arranged parallel to the cell surface, a typical feature of

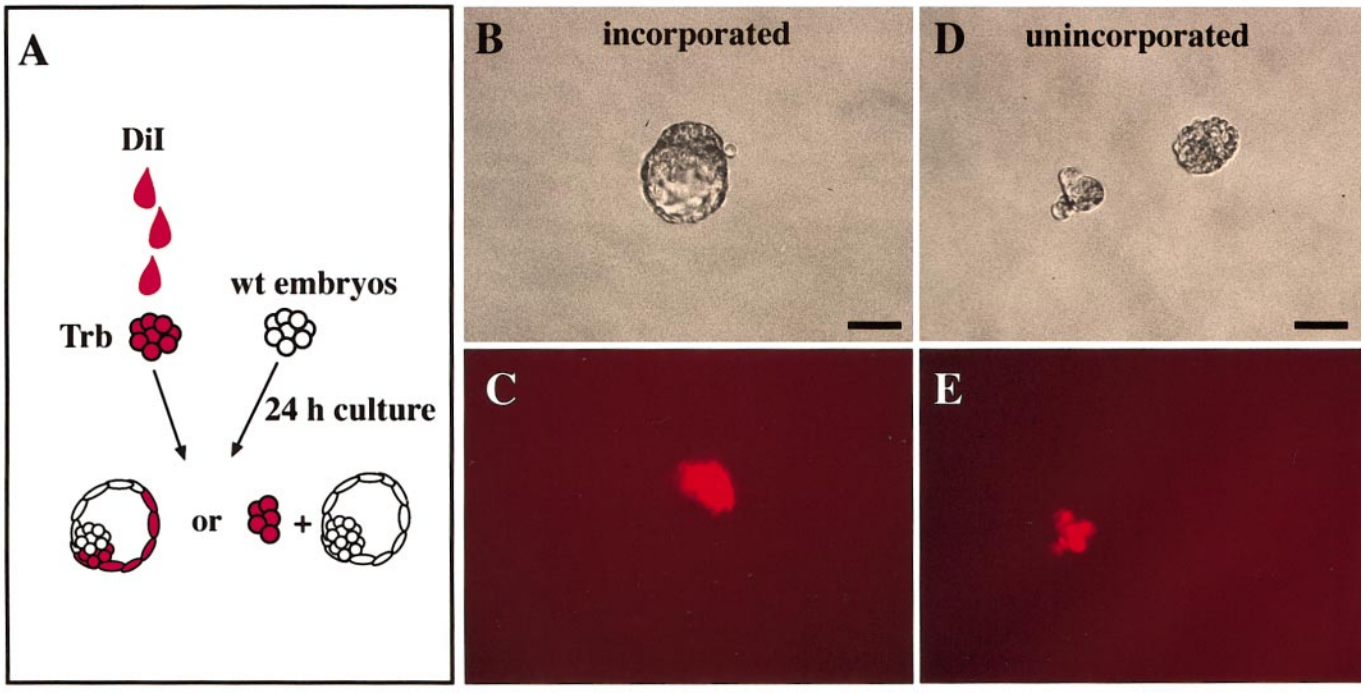

FIG. 7. Chimeric analysis of the mutant phenotype. Embryos from $Trb^{gt/+}$ heterozygous intercrosses were recovered at E2.5, labeled with DiI, aggregated with unlabeled wild-type embryos, and cultured *in vitro* for 1 day. (A) Schematic drawing of the experimental procedure, (B, D) bright-field images, and (C, E) fluorescence image of the two aggregation partners after culture *in vitro.* Note the mutual blastocyst formation of labeled and unlabeled cells that was observed in 78% of all cases (B, C) and the lack of aggregation together with the failure of the labeled aggregation partner to form a blastocyst (D, E) that we observed in 22% of all cases. Bars are 40 μm in B, C, D, and E.

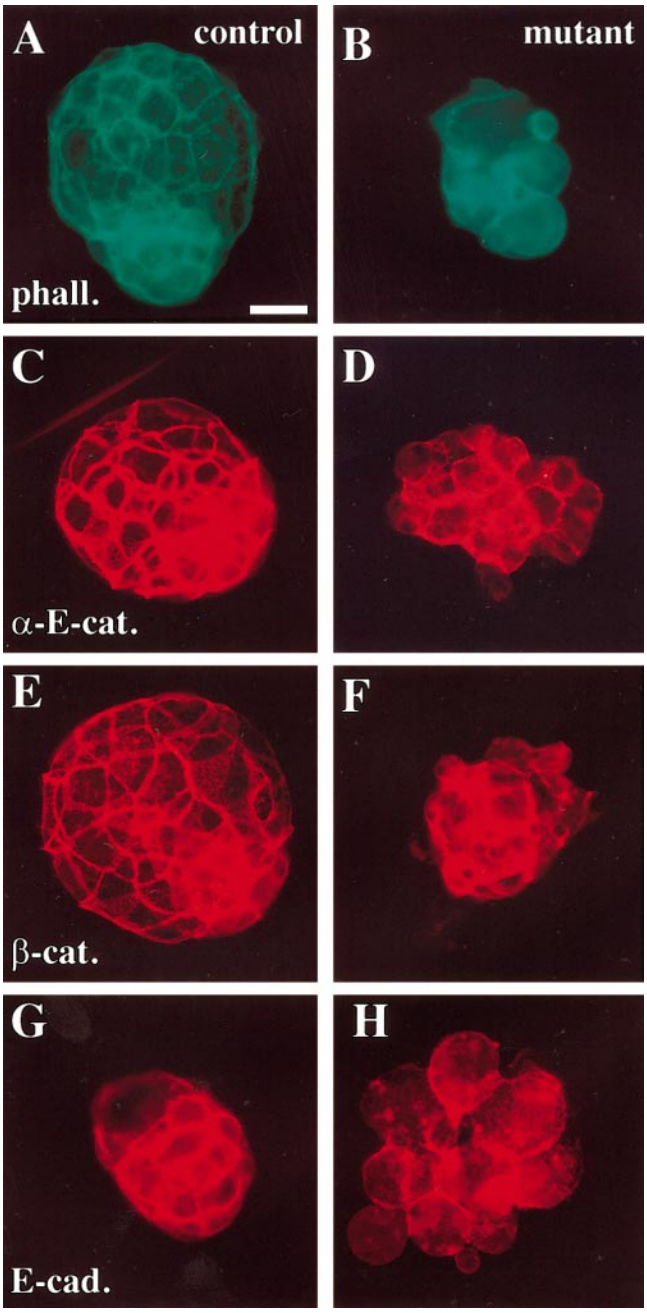

FIG. 8. Immunofluorescence staining of E3.5 embryos of $Trb^{gt/+}$ heterozygous intercrosses for proteins of adhesion complexes and staining for β-actin. (A, B) phalloidin staining for β-actin, (C, D) immunostaining for α-E-catenin, (E, F) for β-catenin, (G, H) for E-cadherin, (A, C, E, G) normal morphology, and (B, D, F, H) mutant morphology. Mutant and control embryos stained strongly for all proteins examined here. Bar is 24 μm in all cases.

compacted blastomeres, were found only in those cells of the mutant embryos that were still compacted, not in the decompacted cells (Fig. 12D). Greatly enlarged secretory vesicles were found in mutant embryos (Fig. 12C), suggesting that secretory vesicles coalesced instead of discharging into the intracellular space as normally happens during blastocoel formation. The structure of the nuclei and nucleoli in E3.5 mutant embryos appeared quite normal if compared to 1 day younger embryos. The nucleoli had the extent of reticular structure typical of compacted morulae. Normal focal cell adhesions, glycogen stores, and mitochondria morphology were observed. From the electron microscopy results we concluded that the *Trb* mutant embryos could have a primary defect in the generation of ribosomes/ribosomal RNA or in translation/transcription in general. In the latter case the paucity of ribosomes would simply be the only product one would expect to be able to see with this method.

DISCUSSION

We have identified a previously undescribed mouse gene, *Traube*, important for murine preimplantation development. In the absence of a fully functional *Trb* gene the homozygous embryos halt in development at the compacted morula stage and die 2 days later after failing to maintain compaction. Chimeric studies showed that the defect was cell autonomous. The *Trb* mutant embryos exhibited reduced cell proliferation. The onset of pathogenesis of the defect occurs after the 8-cell stage and before the fifth cell division, i.e., approximately at the 16-cell stage. Since we observed some mitotic figures in the mutant embryos, it is unlikely that the defect is coupled to a specific number of cell divisions, but rather that the embryos may have failed to develop beyond the point when maternally encoded proteins were no longer sufficient to maintain further development. The presence of very large secretory vesicles was an obvious ultrastructural feature. Smaller secretory vesicles are normally found in the cells of morula stage embryos. These are thought to be the source of the blastocoel fluid (Calarco and Brown, 1969; Cech and Sedlackova, 1983). The development of these very large vesicles in the mutant embryos suggests that the processes forming the vesicles continued to act as in a normal 8- to 16-cell embryo, but that the discharge of the vesicles was impaired. It would appear that the embryos failed to proceed to the next stage of development.

The phenotype of $Trb^{gt/gt}$ embryos resembled that of embryos lacking E-cadherin which also fail to maintain compaction (Larue *et al.*, 1994; Riethmacher *et al.*, 1995). The phenotype of the *Trb* mutant embryos differed in one crucial aspect. In contrast to *Trb* mutant embryos, cells of embryos lacking E-cadherin continue to proliferate (Larue *et al.*, 1994). Embryos expressing a dominant negative FGFR (Chai *et al.*, 1998) also show phenotypic abnormalities similar to those seen in *Trb* mutants. However, analysis of components of the FGF signaling system, of adhesion complexes, tight junctions, and functional analysis of gap junctions indicated that these systems were functional in

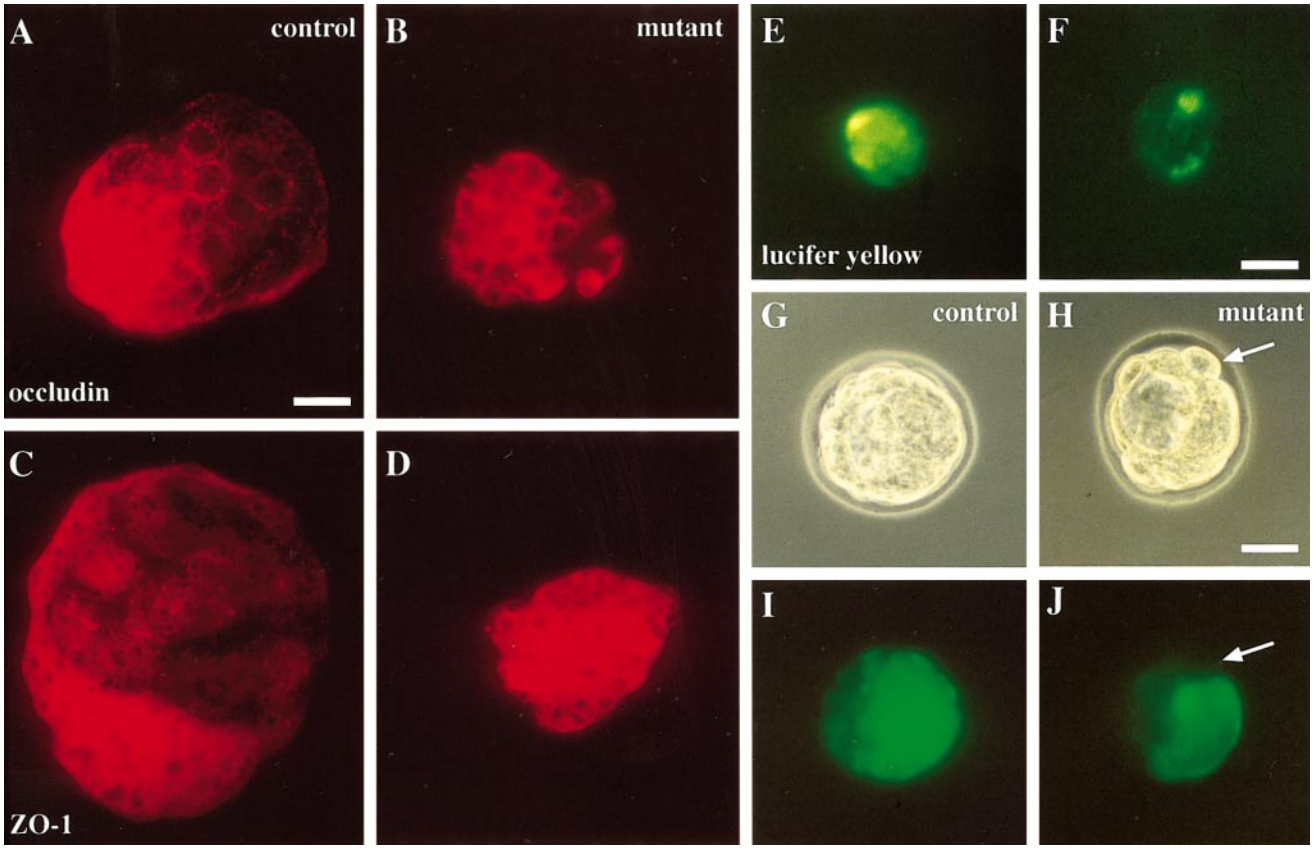

FIG. 9. Immunofluorescence staining of E3.5 embryos of $Trb^{gt/+}$ heterozygous intercrosses for tight junction proteins and functional test of gap junctions. (A, B) Immunostaining for occludin, (C, D) immunostaining for ZO1, (A, C) normal morphology, (B, D) mutant morphology. Mutant and control embryos stained strongly for both proteins examined here. (E, F, G, H, I, J) Embryos injected with the fluorescent dye lucifer yellow, (E, F) Normal morphology of an uncompacted 8-cell-stage embryo (F) and a compacted morula (E) at E2.5, (G, H) Phase contrast images of the embryos shown in I and J, respectively, (G) normal blastocyst, (H) blastocysts with mutant morphology. Lucifer yellow was transported readily to all cells in compacted morulae (E) and little or no dye was transported from one blastomere of uncompacted embryos in the 8-cell stage (F). In normal blastocysts at E3.5 the dye was transported quickly to all cells of the inner cell mass and to all trophectoderm cells (G, I). In mutant embryos dye transfer occurs between cells that were still compacted, but did not occur to cells that had been extruded (arrow in H, J). Bars are 22 μm in A, B, C, and D; 44 μm in E and F; and 36 μm in G, H, I, and J.

Trb mutant embryos, even if retarded in formation at the point of developmental arrest of the *Trb* mutants. We conclude from this that, although the *Trb* mutant phenotype superficially resembles that of embryos lacking functional junctional complexes or FGF signaling pathways, these molecules are not involved in the development of the $Trb^{gt/gt}$ phenotype.

The TRB protein was highly conserved among mice, rats, and humans and contained domains conserved also in a yeast protein. The structure of the TRB protein and its nuclear localization strongly suggest that it is involved in transcription. The TRB-related rat protein, AATF, in combination with a GAL4 DNA-binding domain, has been shown to have transactivation properties on a GAL4 target gene, suggesting that AATF may function as a coactivator of transcription (Page *et al.*, 2000). The observation that the level of *Trb* expression is much higher in some cell types than in others argues against TRB having a general function in transcription.

Expression of *Trb* was ubiquitous early in development, but became progressively more restricted as development proceeded. For example, the *Trb* gene was relatively strongly expressed in the Purkinje cells of the adult cerebellum, but could not be detected above background in other cells of the adult brain. Interestingly, *Trb* starts to be strongly expressed in the liver at the time when the hepatocytes become functionally established. Prior to the differentiation of hepatocytes, blood homeostasis is maintained by the yolk sac (Thomas *et al.*, 1990). From this stage onward the yolk sac becomes increasingly less important as the liver acquires adult functions such as production of plasma proteins (Thomas *et al.*, 1990). This is also a period

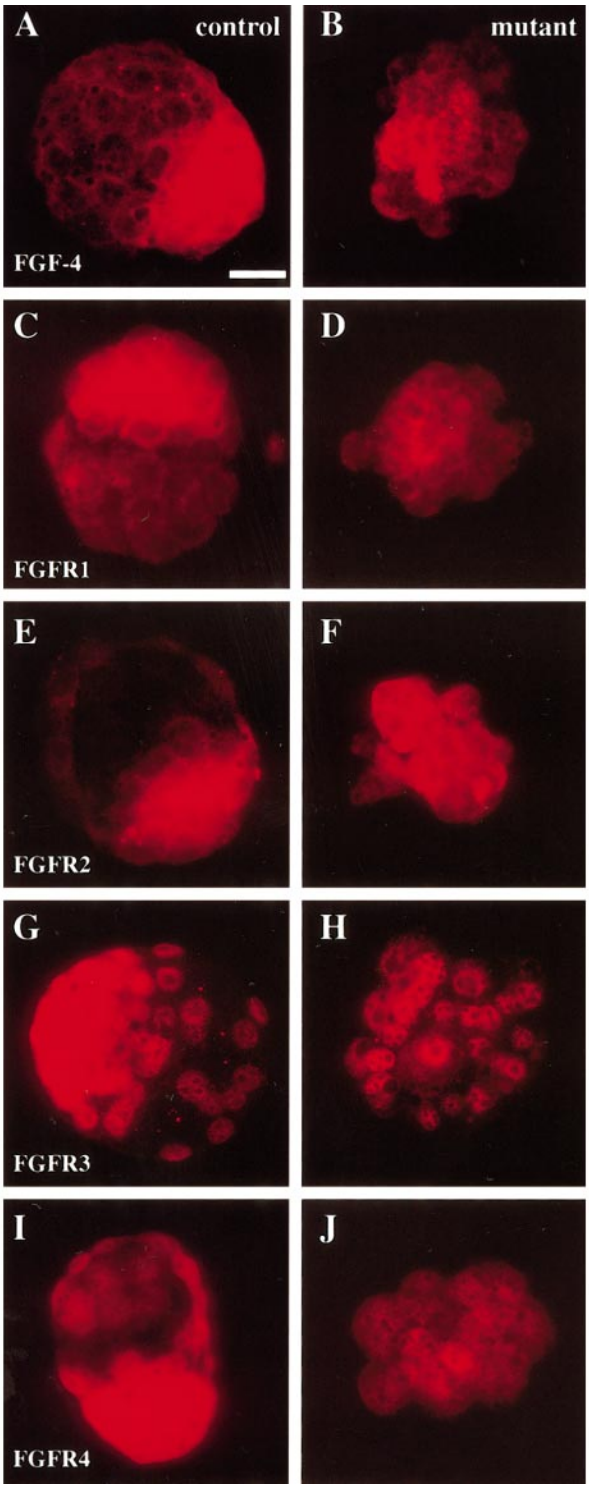

10

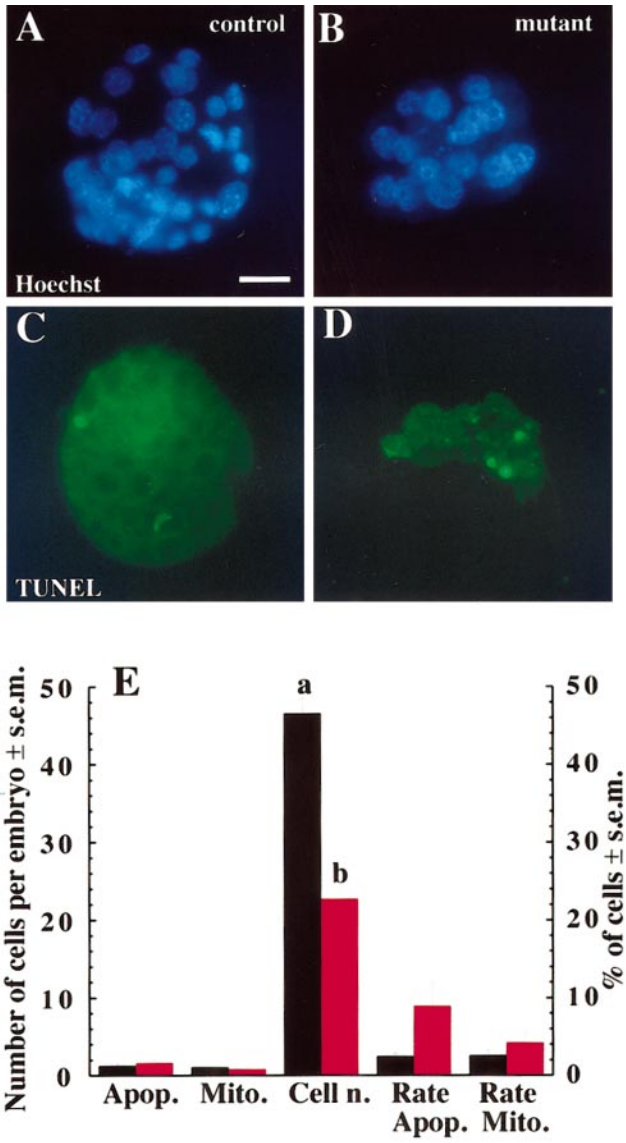

11

FIG. 10. Immunofluorescence staining of E3.5 embryos of *Trb*$^{gt/+}$ heterozygous intercrosses for FGF4 and FGF receptors. (A, B) FGF4, (C, D) FGFR1, (E, F) FGFR2, (G, H) FGFR3, (I, J) FGFR4, (A, C, E, G, I) Normal morphology, and (B, D, F, H, J) mutant morphology. Mutant and control embryos stained strongly for all proteins examined here. Bar is 23 μm in all cases.

FIG. 11. Nuclei staining with Hoechst 33258, TUNEL, and extent of apoptosis and mitosis of E3.5 embryos of *Trb*$^{gt/+}$ heterozygous intercrosses. (A, B) Hoechst 33258 DNA staining, (C, D) TUNEL, (A, C) normal morphology, and (B, D) mutant morphology. (E) Graphical presentation of absolute numbers of apoptotic cells, mitotic cells, and total cell number per embryo as well as rate of apoptosis and mitosis, a $>$ b, $P \leq 0.05$. Note that the cell number was greatly reduced in mutant embryos. The absolute number and the rate of apoptotic and mitotic cells were similar in mutants and controls. Bar is 23 μm in all cases.

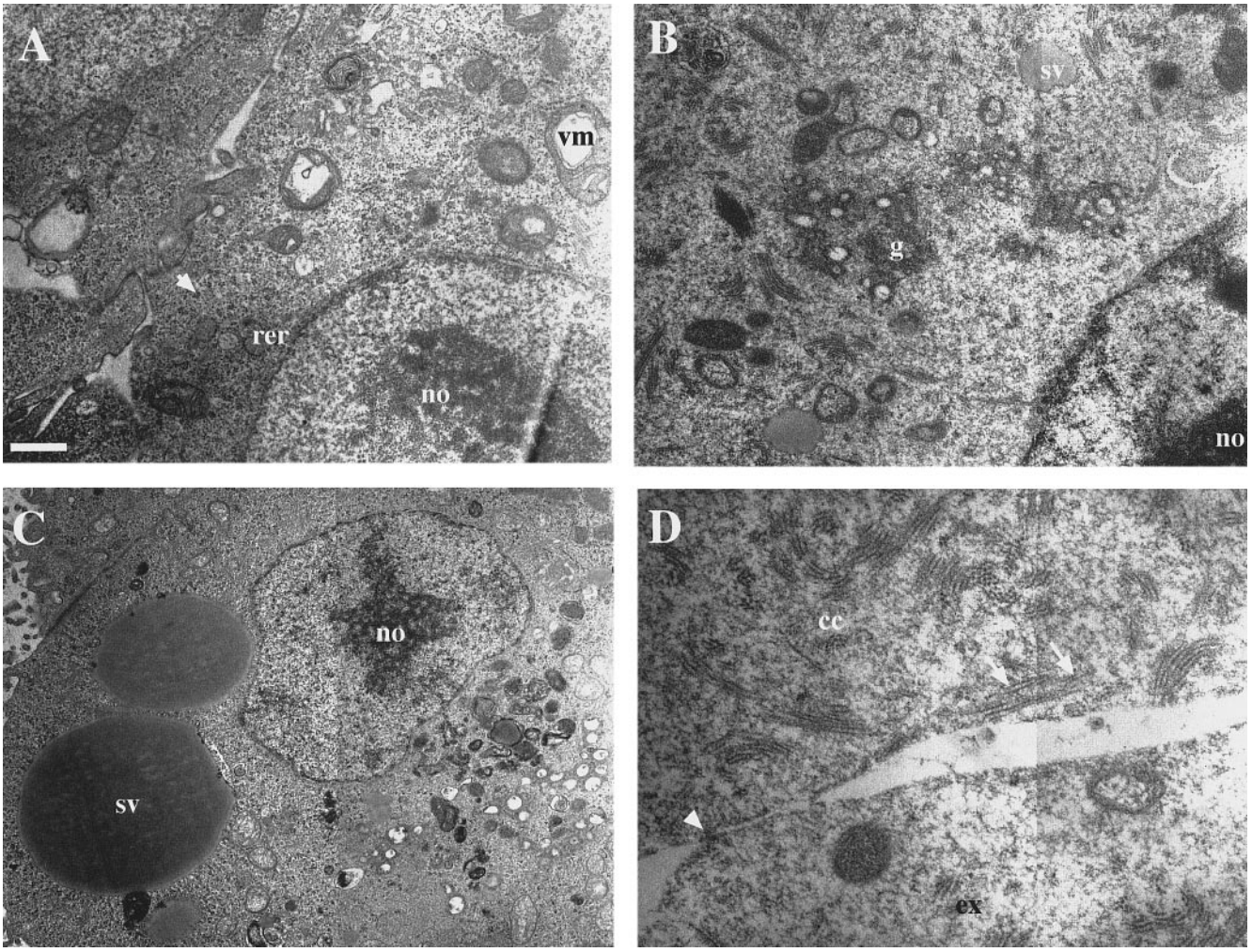

FIG. 12. Transmission electron microscopy of *Trb* mutant embryos. Eighty-nanometer sections of E3.5 embryos of $Trb^{gt/+}$ heterozygous intercrosses. (A) control, (B, C, D) mutant morphology; C is more advanced in the development of the mutant phenotype than B, (D) upper half compacted cell (cc) with extruded cell below (ex). Note abundant free ribosomes and polyribosomes in the cytoplasm of the control (arrow in A) and the paucity of ribosomes and rough endoplasmic reticulum in B. Enlarged secretory vesicles (sv) are visible in C; normal-sized secretory vesicles are visible in B. The structure of the nucleolus in B is less reticulated than the nucleolus in A. Note also the presence of cortical filaments (arrows) in the compacted cell in D and lack of cortical filaments in the extruded cell in D. Focal adhesion points formed in the mutants (arrowhead in D). cc is compacted cell, ex, extruded cell; no, nucleolus; rer, rough endoplasmic reticulum; sv, secretory vesicle; vm, vacuolated mitochondrium. Bar is 480 nm in A and B; and 960 nm in C and D.

of rapid growth of the liver. It should be noted that, although some cells express *Trb* more highly than others, the absolute level of expression is, nevertheless, low compared with mRNA levels coding for other proteins involved in transcription, in particular those which are part of the basal transcriptional apparatus.

The TRB-related rat protein, AATF, was isolated by virtue of its interaction with DLK (DAP-like kinase; Page *et al.*, 2000). DLK, a nuclear protein, is very similar to the Death Associated Protein Kinases (DAP) in the amino-terminal region, including the kinase domain, but lacks a carboxy-terminal death domain. The initial report of DLK suggested that DLK was not involved in regulation of apoptosis (Kogel *et al.*, 1998). However, subsequent reports suggested that DLK (also called ZIP kinase) can induce apoptosis (Kawai *et al.*, 1998). Interaction of AATF with DLK appears to interfere with the induction of apoptosis in a cell culture system (Page *et al.*, 2000). A primary function in regulation of apoptosis is not easily reconciled with the specific expression in the Purkinje cells of the adult cerebellum. The ultrastructure of the *Trb* mutant embryos, TUNEL, and nuclear stain showed no evidence of the nuclear changes accompanying apoptosis. Initially, the embryos halt in development, but they did not die until 48 h

later. Taken together our results suggest that the first essential *in vivo* function of TRB in the mouse does not involve regulation of apoptosis.

Interestingly, the highly acidic amino-terminal region of TRB and TRB-related proteins is found in a number of proteins associated with a chromatin remodeling function during transcription including the MOZ family proteins (Borrow *et al.*, 1996; Champagne *et al.*, 1999) and BRCA1 (Hu *et al.*, 1999). Furthermore, it has been shown that DLK has the potential to phosphorylate a wide variety of substrates including histones (Page *et al.*, 2000). Phosphorylation of histone H3 has been shown to be associated with the condensation of chromosomes during mitosis (Hendzel *et al.*, 1997). In contrast, phosphorylation of histone H1, which is not dependent on a particular stage of the cell cycle, is associated with transcriptional activation (Lee and Archer, 1998). An essential feature of embryonic genome activation is chromatin remodeling, since both the maternal and the paternal genomes are in an inactive state after fertilization (reviewed by Latham, 1999). Possibly, an interaction between TRB and DLK, involving a function of DLK unrelated to apoptosis, is necessary for perimplantation development.

We observed that in a large percentage of cells transfected with a 5 myc epitope-tagged *Trb* coding sequence that the TRB/5MYC protein was localized to nucleoli. The observation that TRB was not always found in the nucleoli may indicate that TRB may be important in the nucleoli in a particular stage in the cell cycle. The structure of the nucleolus changes throughout the cell cycle. During mitosis the chromosomes condense and no nucleolus is present. After mitosis active transcription of the rRNA genes starts and several nucleoli develop in the vicinity of chromosomal regions containing the rRNA genes. In most cells these nascent nucleoli fuse to form one single nucleolus. Other cell types, including the COS7 cells used in our experiment, retain more than one nucleolus. The ultrastructure of the nucleolus changes during preimplantation development from a fibrillar condensed to a more open reticular structure (Hillman and Tasca, 1969). The nucleoli of embryos exhibiting the $Trb^{gt/gt}$ phenotype at E3.5 were developed normally for a compacting 8-cell stage embryo (Hillman and Tasca, 1969), but retarded for an E3.5 embryo. The early stages of embryonic gene activation must be performed using maternally encoded proteins and regulation of this process occurs at the posttranscriptional level (Latham, 1999). Prior to the establishment of embryonic transcription chromatin structure is organized using histones translated from maternal mRNA (Wiekowski *et al.*, 1997). Therefore, it is possible that the ultrastructure of the nucleus initially develops normally, due to maternally encoded proteins. Only after embryonic gene activation do embryos synthesize histones and concomitantly acquire the ability to activate and repress transcription (Wiekowski *et al.*, 1997).

The synthesis of embryonic RNA increases dramatically between the 8-cell stage and the blastocyst, since large numbers of ribosomes are required to produce proteins essential for subsequent development. Even a modest reduction in the efficiency of the nucleoli may have fatal consequences (reviewed by Johnson, 1981). Accordingly, the number of free ribosomes, polyribosomes, and rough endoplasmic reticulum increases (Calarco and Brown, 1969; Hillman and Tasca, 1969). The dominant ultrastructural feature of the E3.5 *Trb* mutant embryos was the paucity of ribosomes, polyribosomes, and rough endoplasmic reticulum which was even prominent when compared to 8-cell stage embryos (Calarco and Brown, 1969). This possibly indicates that the mutant embryos failed to maintain adequate levels of transcription to support further development in the absence of maternal mRNA stores.

In conclusion, we have identified a gene essential for the earliest phase of mouse development. The nature of the phenotype together with the observation that *Trb* is a nuclear protein suggests that this protein may be involved in one or more aspects of the embryo establishing genetic control of its own development.

ACKNOWLEDGMENTS

We gratefully appreciate the excellent technical assistance of Marion Stäger, Victor Diaz, Gudrun Weinrich, and Andrea Conrad. We thank Dieter Koetting for help with the electron microscopy and Ulli Francke for microinjection. We thank W. Skarnes for providing pGT1.8geo and L. Schalkwyk for providing information regarding the genomic localization of *Che1* and *Ded*. A.K.V. was supported by a fellowship of the Deutsche Forschungsgemeinschaft. T.T. was supported by an EMBO fellowship. This research was funded by AmGen Inc. and the Max Planck Society.

REFERENCES

Arman, E., Haffner-Krausz, R., Chen, Y., Heath, J., and P. L. (1998). Targeted disruption of fibroblast growth factor (FGF) receptor 2 suggests a role for FGF signaling in pregastrulation mammalian development. *Proc. Natl. Acad. Sci. USA* **95,** 5082–5087.

Becker, D., Leclerc-David, C., and Warner, A. (1992). The relationship of gap junctions and compaction in the preimplantation mouse embryo. *Development* (Suppl.), 113–118.

Bornberg-Bauer, E., Rivals, E., and Vingron, M. (1998). Computational approaches to identify leucine zippers. *Nucleic Acids Res.* **26,** 2740–2746.

Borrow, J., Stanton, V. J., Andresen, J., Becher, R., Behm, F., Chaganti, R., Civin, C., Disteche, C., Dube, I., Frischauf, A., Horsman, D., Mitelman, F., Volinia, S., Watmore, A., and Housman, D. (1996). The translocation t(8;16)(p11;p13) of acute myeloid leukemia fuses a putative acetyltransferase to the CREB-binding protein. *Nature Genet.* **14,** 33–41.

Calarco, P. G., and Brown, E. H. (1969). An ultrastructural and cytological study of preimplantation development of the mouse. *J. Exp. Zool.* **171,** 253–283.

Cech, S., and Sedlackova, M. (1983). Ultrastructure and morphometric analysis of preimplantation mouse embryos. *Cell Tissue Res.* **230,** 661–670.

Chai, N., Patel, Y., Jacobson, K., McMahon, J., McMahon, A., and Rappolee, D. (1998). FGF is an essential regulator of the fifth cell

division in preimplantation mouse embryos. *Dev. Biol.* **198,** 105–115.

Champagne, N., Bertos, N., Pelletier, N., Wang, A., Vezmar, M., Yang, Y., Heng, H., and Yang, X.-J. (1999). Identification of a human histone acetyltransferase related to monoctic leukemia zinc finger protein. *J. Biol. Chem.* **274,** 28528–28536.

Cheng, S., and Constantini, F. (1993). Morula decompaction (mdm), a preimplantation recessive lethal defect in a transgenic mouse line. *Dev. Biol.* **156,** 265–277.

Ducibella, T., and Anderson, E. (1975). Cell shape and membrane changes in the eight cell mouse embryo: Prerequisites for morphogenesis of the blastocyst. *Dev. Biol.* **47,** 45–58.

Ekblom, P., Vestweber, D., and Kemler, R. (1986). Cell-matrix interactions and cell adhesion during development. *Annu. Rev. Cell Biol.* **2,** 27–47.

Feldman, B., Poueymirou, W., Papaioannou, V. E., DeChiara, T. M., and Goldfarb, M. (1995). Requirement of FGF-4 for postimplantation mouse development. *Science* **267,** 246–249.

Flach, G., Johnson, M., Braude, P., Taylor, R., and Bolton, V. (1982). The transition from maternal to embryonic control in the 2-cell mouse embryo. *EMBO J.* **1,** 681–686.

Haffner-Krausz, R., Gorivodsky, M., Chen, Y., and Lonai, P. (1999). Expression of Fgfr2 in the early mouse embryo indicates its involvement in preimplantation development. *Mech. Dev.* **85,** 167–172.

Hendzel, M., Wei, Y., Mancini, M., Van Hooser, A., Ranalli, T., Brinkley, B., Bazett-Jones, D., and CD.,A. (1997). Mitosis-specific phosphorylation of histone H3 initiates primarily within pericentromeric heterochromatin during G2 and spreads in an ordered fashion coincident with mitotic chromosome condensation. *Chromosoma* **106,** 348–360.

Hillman, N., and Tasca, R. J. (1969). Ultrastructural and autoradiographic studies of mouse cleavage stages. *Am. J. Anat.* **126,** 151–173.

Hogan, B., Beddington, R., Constantini, F., and Lacy, E. (1994). "Manipulating the Mouse Embryo: A Laboratory Manual." Cold Spring Harbor Laboratory Press, Cold Spring Harbor, NY.

Hu, Y., Hao, Z., and Li, R. (1999). Chromatin remodeling and activation of chromosomal DNA replication by an acidic transcriptional activation domain from BRCA1. *Gen. Dev.* **13,** 637–642.

Johnson, M. (1981). The molecular and cellular basis of preimplantation mouse development. *Biol. Rev.* **56,** 463–498.

Johnston, C., Cox, H., Gomm, J., and Coombes, R. (1995). Fibroblast growth factor receptors (FGFRs) localize in different cellular compartments. A splice variant of FGFR-3 localizes to the nucleus. *J. Biol. Chem.* **270,** 30643–30650.

Kawai, T., Matsumoto, M., Takeda, K., Sanjo, H., and Akira, S. (1998). ZIP kinase, a novel serine/threonine kinase which mediates apoptosis. *Mol. Cell. Biol.* **18,** 1642–1651.

Kelly, S. (1977). Studies on the development potential of 4- and 8-cell stage embryos. *J. Exp. Zool.* **200,** 365–376.

Kemler, R. (1993). From cadherins to catenins: Cytoplasmic protein interactions and regulation of cell adhesion. [Review] *Trends Genet.* **9,** 317–321.

King, R. D., and Sternberg, M. J. (1996). Identification and application of the concepts important for accurate and reliable protein secondary structure prediction. *Protein Sci.* **5,** 2298–2310.

Koch, P. J., Mahoney, M. G., Ishikawa, H., Pulkkinen, L., Uitto, J., Shultz, L., Murphy, G. F., Whitaker-Menezes, D., and Stanley, J. R. (1997). Targeted disruption of the pemphigus vulgaris antigen (desmoglein 3) gene in mice causes loss of keratinocyte cell adhesion with a phenotype similar to pemphigus vulgaris. *J. Cell Biol.* **137,** 1091–1102.

Kogel, D., Plottner, O., Landsberg, G., Christian, S., and Scheidtmann, K. (1998). Cloning and characterization of Dlk, a novel serine/threonine kinase that is tightly associated with chromatin and phosphorylates core histones. *Oncogene* **17,** 2645–2654.

Kozak, M. (1989). The scanning model for translation: An update. *J. Cell Biol.* **108,** 229–241.

Larue, L., Ohsugi, M., Hirchenhain, J., and Kemler, R. (1994). E-cadherin null mutant embryos fail to form a trophectoderm epithelium. *Proc. Natl. Acad. Sci. USA* **91,** 8263–8267.

Latham, K. (1999). Mechanisms and control of embryonic genome activation in mammalian embryos. *Int. Rev. Cytol.* **193,** 71–124.

Lee, H., and Archer, T. (1998). Prolonged glucocorticoid exposure dephosphorylates histone H1 and inactivates the MMTV promoter. *EMBO J.* **17,** 1454–1466.

Lee, S., Gilula, N., and Warner, A. (1987). Gap junctional communication and compaction during preimplantation stages of mouse development. *Cell* **51,** 851–860.

Magnuson, T., and Epstein, C. (1981). Genetic control of very early mammalian development. *Biol. Rev.* **56,** 369–408.

Nagy, A., and Rossant, J. (1993). Production of completely ES cell-derived fetuses. In "Gene Targeting. A Practical Approach" (A. L. Joyner, Ed.), pp. 147–178. IRL Press, Oxford.

Page, G., Lodige, I., Kogel, D., and Scheidtmann, K. (2000). AATF, a novel transcription factor that interacts with Dlk/ZIP kinase and interferes with apoptosis. *FEBS Lett.* **462,** 187–191.

Rappolee, D., Basilico, C., Patel, Y., and Werb, Z. (1994). Expression and function of FGF-4 in peri-implantation development in mouse embryos. *Development* **120,** 2259–2269.

Rappolee, D., Patel, Y., and Jacobson, K. (1998). Expression of fibroblast growth factor receptors in peri-implantation mouse embryos. *Mol. Reprod. Dev.* **51,** 254–264.

Riethmacher, D., Brinkmann, V., and Birchmeier, C. (1995). A targeted mutation in the mouse E-cadherin gene results in defective preimplantation development. *Proc. Natl. Acad. Sci. USA* **92,** 855–859.

Roth, M. B., Zahler, A. M., and Stolk, J. A. (1991). A conserved family of nuclear phosphoproteins localized to sites of polymerase II transcription. *J. Cell Biol.* **115,** 587–896.

Ruiz, P., Brinkmann, V., Ledermann, B., Behrend, M., Grund, C., Thalhammer, C., Vogel, F., Birchmeier, C., Gunthert, U., Franke, W. W., and Birchmeier, W. (1996). Targeted mutation of plakoglobin in mice reveals essential functions of desmosomes in the embryonic heart. *J. Cell Biol.* **135,** 215–225.

Skarnes, W. C., Moss, J. E., Hurtley, S. M., and Beddington, R. S. (1995). Capturing genes encoding membrane and secreted proteins important for development. *Proc. Natl. Acad. Sci. USA* **92,** 6592–6596.

Thomas, T., Southwell, B., Schreiber, G., and Jaworowski, A. (1990). Plasma protein synthesis and secretion in the rat visceral yolk sac. *Placenta* **11,** 414–430.

Thomas, T., Voss, A. K., and Gruss, P. (1998). Distribution of a murine protein tyrosine phosphatase BL-β-galactosidase fusion protein suggests a role in neurite out growth. *Dev. Dynam.* **212,** 250–257.

Thompson, J. D., Higgins, D. G., and Gibson, T. J. (1994). CLUSTAL W: Improving the sensitivity of progressive multiple sequence alignment through sequence weighting, position-specific gap penalties and weight matrix choice. *Nucleic Acids Res.* **22,** 4673–4680.

Torres, M., Stoykova, A., Huber, O., Chowdhury, K., Bonaldo, P., Mansouri, A., Butz, S., Kemler, R., and Gruss, P. (1997). An alpha-E-catenin gene trap mutation defines its function in preimplantation development. *Proc. Natl. Acad. Sci. USA* **94,** 901–906.

Voss, A. K., Thomas, T., and Gruss, P. (1997). Germ line chimeras from female ES cells. *Exp. Cell Res.* **230,** 45–49.

Voss, A. K., Thomas, T., and Gruss, P. (1998a). Compensation for a gene trap mutation in the microtubule associated protein 4 locus by alternative polyadenylation and alternative splicing. *Dev. Dynam.* **212,** 258–266.

Voss, A. K., Thomas, T., and Gruss, P. (1998b). Efficiency assessment of the gene trap approach. *Dev. Dynam.* **212,** 171–180.

Wiekowski, M., Miranda, M., Nothias, J.-Y., and DePamphilis, M. (1997). Changes in histone synthesis and modification at the beginning of mouse development correlate with the establishment of chromatin mediated repression of transcription. *J. Cell Sci.* **110,** 1147–1158.

Received for publication March 3, 2000
Revised August 27, 2000
Accepted August 27, 2000
Published online October 20, 2000